Supporting Information

A low cost mobile phone dark-field microscope for nanoparticle-based quantitative studies

Dali Sun [a], *Tony Y. Hu* [a*]
[a] School of Biological and Health Systems Engineering, Virginia G. Piper Biodesign Center for Personalized Diagnostics, The Biodesign Institute, Arizona State University, 727 E. Tyler St. B 130-B, Tempe, AZ 85287, United States.

Corresponding author. Fax: + 1 480-965-3051; Tel.:+ 1 480-727-1880; E-mail address: tyhu@asu.edu

Table of contents

Experimental Section

Exosome quantification assay.

The AuNR probe was generated by adding 40 µL of neutravidin-labeled AuNRs (Nanopartz C12-25-650-TN-50, 7×10-9 M) to 200 µL PBS, then added 20 µL biotinylated CD9 antibody (NB110-81616, Novus, 0.5mg/mL), and sonicated the mixture for 8 minutes at 80% amplitude using a 5 second on/off cycle (Q500 Sonicator, Qsonica) to accelerate conjugation. AuNR samples were then centrifuged at 4000× g for 10 min, aspirated, resuspended in 400 µL PBS and washed twice more using the same protocol, then resuspended in 200 µL PBS and stored at 4°C until use. Protein A/G-modified 192-well slides (Arrayit) were incubated with 1 µL/well anti-LAM IgG (courtesy of BEI Resources) and sonicated at 37.5°C for 8 minutes at 80% amplitude using a 5 second on/off cycle (Q500 Sonicator, Qsonica) to accelerate IgG binding. Slides were then blocked with 1 µL/well 5% BSA (Thermo Scientific) for 1 hour at 37.5°C and PBS-washed 3 times before use. Slides were loaded with 1 µL/well of 2-fold PBS-diluted serum, PBS-washed times, and incubated with anti-CD9 IgG-conjugated-AuNRs for 1 hour at 37.5°C in a humidified chamber, then washed for 10 min at 25°C with PBS and 0.01% Tween-20 (PBST, pH 7.0), rinsed with deionized water, and air-dried for DFM imagery.

Tables

Table S1. Cost list of the MDFM.

Item	Supplier	Cost ($)
Objective Lens (10×/20×)*	Olympus	200 / 400
Condenser	Olympus	920
Case	3dhubs.com	60
Mobile Phone	Motorola	180
	Total	1360 / 1560

* Lens details in Table S3

Table S2. MDFM and DDFM inter-assay and intra-assay reproducibility.

Assay	Concentration μg/μL	Precision (% CV)			
		Inter-assay		Intra-assay	
		MDFM	DDFM	MDFM	DDFM
Binding affinity	0.091	13.65	5.51	5.11	5.52
	0.023	11.69	3.86	3.76	4.20
	0.005	9.83	3.89	3.20	1.60
Protein quantification	0.083	8.06	6.02	3.06	2.14
	0.021	10.89	5.74	7.37	2.30
	0.005	13.32	8.02	7.79	7.72

Table S3. Objective lens specification for MDFM.

	10×	20×
Manufacturer	Olympus	Olympus
Model	CACHN10XPHP	LCACHN20XPHP
Numerical Aperture	0.25	0.4
Working Distance (mm)	8.8	3.2
F Number	22	22

Table S4. Demographic and Clinical data of the exosome analysis cohort. The HTI cohort that served as a source of case and control samples in this study were the subjects of a large, population-based TB surveillance study that performed active surveillance of all confirmed TB cases in Houston/Harris County, Texas between 1995 and 2004.

Group	Labels	Age	Gender	TB Diagnosis	Culture Positive	Skin Test Positive
TB	1153.01	16	M	Yes	No	Yes
	1150.01	13	F	Yes	No	Yes
	1133.01	17	M	Yes	Yes	Yes
	1121.01	9	M	Yes	No	Yes
	1109.01	16	F	Yes	Yes	Yes
Healthy	1113.05	9	M	No	N/A	N/A
	1139.04	17	F	No	N/A	N/A
	1076.10	11	M	No	N/A	N/A
	1170.05	8	F	No	N/A	N/A
	1182.04	4	F	No	N/A	N/A

Table S5 Summery of mobile phone microscope studies.

#	***Researchers***	***Target***	***Application***	***Illumination***	***Field***
	Pathogens				
1	(Pirnstill and Coté, 2015)	Malaria parasites	I	BF	NF
2	(Koydemir et al., 2015)	Giardia parasites	I & Q	BF	FF
3	(D'Ambrosio et al., 2015)	Filarial parasites	I & Q	BF	FF
4	(Ame et al., 2013)	Helminth parasites	I	BF	FF
	Cells				
5	(Phillips et al., 2015)	Cells	I	BF & DF	FF
6	(Switz et al., 2014)	Epithelial cell	I	BF	FF
7	(Skandarajah et al., 2014)	Red blood cells	I & Q	BF	FF
8	(Lee and Yang, 2014)	Cells	I	BF	FF
9	(Breslauer et al., 2009)	Blood cells	I	BF	FF
	Biomolecules				
10	(Wang et al., 2017)	BSA	I & Q	BF	FF
11	(Archibong et al., 2017)	Hemoglobin	I & Q	BF	FF
12	(Lee et al., 2017)	estradiol	I & Q	BF	FF
13	(Khan et al., 2015)	Glucose	Q	BF	FF
14	(Berg et al., 2015)	HSV-1 IgG	Q	BF	FF
15	(Lee et al., 2011)	DNA	Q	BF	FF
16	(Zhang et al., 2011)	DNA	I & Q	BF	FF
	Particles				

17	(Wei et al., 2013)	Fluorescent particle	I & Q	BF	NF
18	(Preechaburana et al., 2011)	Gold Particle	I & Q	BF	FF
19	(Lu et al., 2009)	Gold Particle	I & Q	BF	FF

I: imaging; Q: quantification; BF: bright-field; DF: dark-field; NF: near-field; Far-field: FF

Figures

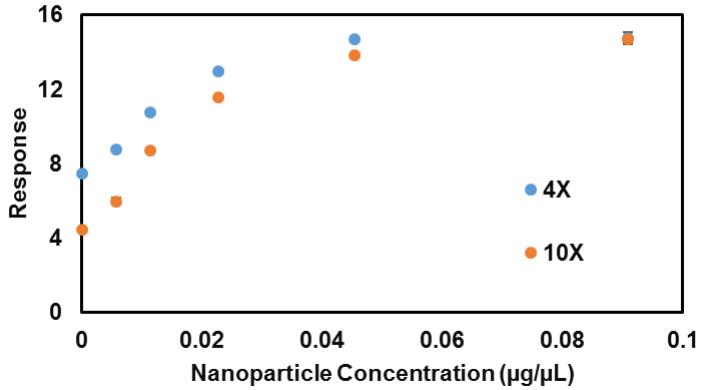

Figure S1. DSM response comparison of different magnification (4X and 10X objective lens) under DFM high resolution (4080x3072 px) for binding affinity assay same as shown in Figure 4a.

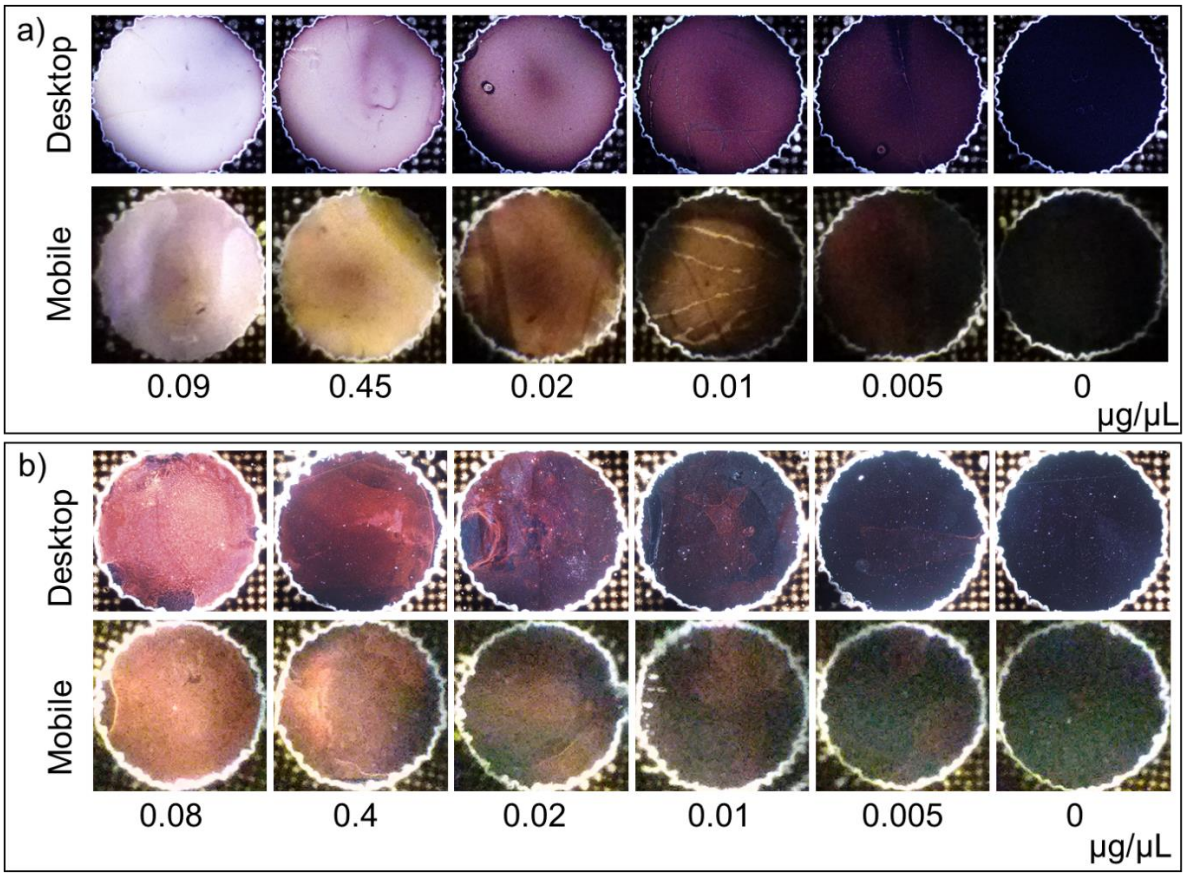

Figure S2. Representative images by MDFM and DDFM for a) binding affinity assay (b) protein quantification assay along with nanoparticle and target concentration gradient respectively.

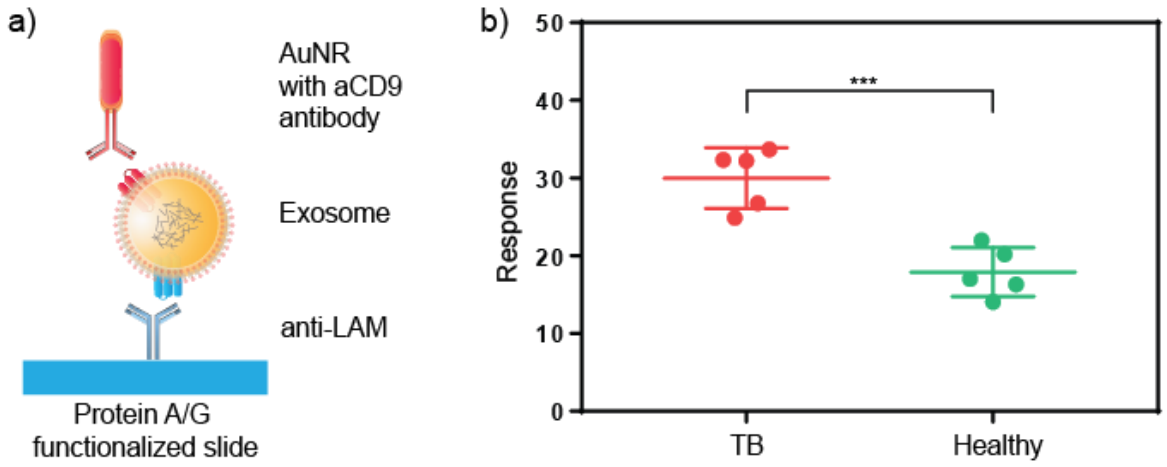

Figure S3. Exosome quantification scheme. Antibody-labeled detection wells bind exosomes derived from cells that have internalized *Mycobacterium tuberculosis* (*Mtb*) bacilli by binding the *Mtb* antigen lipoarabinomannan (LAM). These *Mtb*-derived exosomes are mixed with a nanoparticle-labeled probe that binds CD9, a pan-specific exosome biomarker, and quantified by DFM image analysis. (b) DSM-quantified *Mtb* exosome concentrations in serum samples of pediatric patients with tuberculosis (TB) and healthy controls. Data are presented as mean ± SEM, N=5/group; ***p=0.0007 by two-sided Mann-Whitney U-test. Table S4 is the demographic information of the cohort.

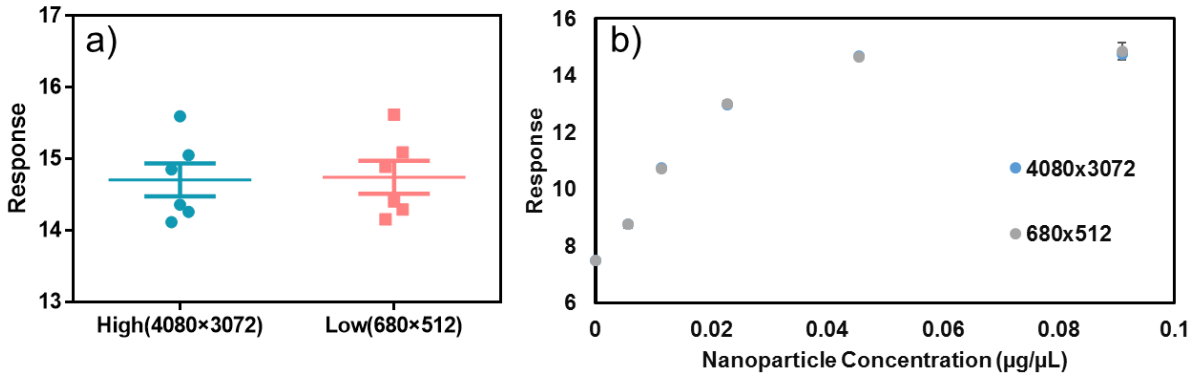

Figure S4. Comparison of quantification results from high (4080x3072) and low (680x512) resolution DDFM images at (a) a single concentration point (0.023 μg/μL) and (b) across multiple concentration values (0 μg/μL to 0.09 μg/μL) for the assay scheme depicted in Figure 4a. Graphs depict Mean ± SD values for each concentration value. The mean ratios of paired low-resolution to high-resolution response values for a) and b) were 0.9976 ± 0.0005 and 0.9992 ± 0.0036, respectively.

Reference

Ame, S.M., Ali, S.M., Keiser, J., Bogoch, I.I., Andrews, J.R., Speich, B., 2013. Short Report : Mobile Phone Microscopy for the Diagnosis of Soil-Transmitted Helminth Infections : A Proof-of-Concept Study 88, 626–629. doi:10.4269/ajtmh.12-0742

Archibong, E., Konnaiyan, K.R., Kaplan, H., Pyayt, A., 2017. A mobile phone-based approach to detection of hemolysis. Biosens. Bioelectron. 88, 204–209. doi:10.1016/j.bios.2016.08.030

Berg, B., Cortazar, B., Tseng, D., Ozkan, H., Feng, S., Wei, Q., Chan, R.Y.L., Burbano, J., Farooqui, Q., Lewinski, M., Di Carlo, D., Garner, O.B., Ozcan, A., 2015. Cellphone-Based Hand-Held Microplate Reader for Point-of-Care Testing of Enzyme-Linked Immunosorbent Assays. ACS Nano 9, 7857–7866. doi:10.1021/acsnano.5b03203

Breslauer, D.N., Maamari, R.N., Switz, N.A., Lam, W.A., Fletcher, D.A., 2009. Mobile phone based clinical microscopy for global health applications. PLoS One 4, 1–7. doi:10.1371/journal.pone.0006320

D'Ambrosio, M. V., Bakalar, M., Bennuru, S., Reber, C., Skandarajah, A., Nilsson, L., Switz, N., Kamgno, J., Pion, S., Boussinesq, M., Nutman, T.B., Fletcher, D.A., 2015. Point-of-care quantification of blood-borne filarial parasites with a mobile phone microscope. Sci. Transl. Med. 7, 286re4-286re4. doi:10.1126/scitranslmed.aaa3480

Khan, S.A., Smith, G.T., Seo, F., Ellerbee, A.K., 2015. Label-free and non-contact optical biosensing of glucose with quantum dots. Biosens. Bioelectron. 64, 30–35. doi:10.1016/j.bios.2014.08.035

Koydemir, H.C., Gorocs, Z., Tseng, D., Cortazar, B., Feng, S., Chan, R.Y.L., Burbano, J., McLeod, E., Ozcan, A., 2015. Rapid imaging, detection and quantification of Giardia lamblia cysts using mobile-phone based fluorescent microscopy and machine learning. Lab Chip 15, 1284–1293. doi:10.1039/C4LC01358A

Lee, D., Chou, W.P., Yeh, S.H., Chen, P.J., Chen, P.H., 2011. DNA detection using commercial mobile phones. Biosens. Bioelectron. 26, 4349–4354. doi:10.1016/j.bios.2011.04.036

Lee, S.A., Yang, C., 2014. A smartphone-based chip-scale microscope using ambient illumination. Lab Chip 14, 3056–3063. doi:10.1039/c4lc00523f

Lee, W.-I., Shrivastava, S., Duy, L.-T., Yeong Kim, B., Son, Y.-M., Lee, N.-E., 2017. A smartphone imaging-based label-free and dual-wavelength fluorescent biosensor with high sensitivity and accuracy. Biosens. Bioelectron. 94, 643–650. doi:10.1016/j.bios.2017.03.061

Lu, Y., Shi, W., Qin, J., Lin, B., 2009. Low cost, portable detection of gold nanoparticle-labeled microfluidic immunoassay with camera cell phone. Electrophoresis 30, 579–582. doi:10.1002/elps.200800586

Phillips, Z.F., D'Ambrosio, M. V., Tian, L., Rulison, J.J., Patel, H.S., Sadras, N., Gande, A. V., Switz, N.A., Fletcher, D.A., Waller, L., 2015. Multi-contrast imaging and digital refocusing on a mobile microscope with a domed LED array. PLoS One 10, 1–13. doi:10.1371/journal.pone.0124938

Pirnstill, C.W., Coté, G.L., 2015. Malaria Diagnosis Using a Mobile Phone Polarized Microscope. Sci. Rep. 1–13. doi:10.1038/srep13368

Preechaburana, P., Macken, S., Suska, A., Filippini, D., 2011. HDR imaging evaluation of a NT-proBNP test with a mobile phone. Biosens. Bioelectron. 26, 2107–2113. doi:10.1016/j.bios.2010.09.015

Skandarajah, A., Reber, C.D., Switz, N.A., Fletcher, D.A., 2014. Quantitative Imaging with a Mobile Phone Microscope 9. doi:10.1371/journal.pone.0096906

Switz, N.A., Ambrosio, M.V.D., Fletcher, D.A., 2014. Low-Cost Mobile Phone Microscopy with a Reversed Mobile Phone Camera Lens 9. doi:10.1371/journal.pone.0095330

Wang, L.J., Chang, Y.C., Sun, R., Li, L., 2017. A multichannel smartphone optical biosensor for high-throughput point-of-care diagnostics. Biosens. Bioelectron. 87, 686–692. doi:10.1016/j.bios.2016.09.021

Wei, G.Q., Qi, H., Luo, W., Tseng, D., Ki, S.J., Wan, Z., Bentolila, L.A., Wu, T., Sun, R., Ozcan, A., Pharmacology, M., Angeles, L., States, U., 2013. Fluorescent Imaging of Single Nanoparticles and Viruses on a Smart Phone 9147–9155.

Zhang, G., Li, C., Lu, Y., Hu, H., Xiang, G., Liang, Z., Liao, P., Dai, P., Xing, W., Cheng, J., 2011. Validation of a mobile phone-assisted microarray decoding platform for signal-enhanced mutation detection. Biosens. Bioelectron. 26, 4708–4714. doi:10.1016/j.bios.2011.05.031